European Journal of Neuroscience, Vol. 8, pp. 1853–1864, 1996

Plasticity of Metabolic Whisker Maps in Somatosensory Brainstem and Thalamus of Mice with Neonatal Lesions of Whisker Follicles

Peter Melzer and Carolyn B. Smith
Laboratory of Cerebral Metabolism, National Institute of Mental Health, Building 36, Room 1A05, 9000 Rockville Pike, Bethesda, MD 20892, USA

Keywords: neonatal plasticity, mouse, trigeminal brainstem, thalamic ventrobasal complex, quantitative autoradiographic deoxyglucose method

Abstract

We employed the autoradiographic deoxyglucose method to study metabolic whisker maps of the adult mouse somatosensory brainstem and thalamus after the neonatal removal of left whisker follicles C1, C2 and C3. Left whiskers B1–3 and D1–3 were deflected to metabolically activate the somatosensory pathway. Unoperated mice that were stimulated in the same fashion served as controls. Whisker stimulation resulted in an ipsilateral increase in metabolic activity in the three trigeminal brainstem structures in which the whiskers are represented topologically by segments of high cytochrome oxidase activity, i.e. subnucleus caudalis, subnucleus interpolaris and nucleus principalis. In the two subnuclei of mice with lesions and of controls, there was an increase in metabolic activity of the representations of the deflected whiskers, whereas the metabolic activity of representations A1–3 and E1–3 was low. Apart from these similarities, the metabolic activation of the representations originally representing whiskers C1–3 was remarkably greater in mice with lesions than in controls. This increase reached statistical significance in subnucleus caudalis and approached statistical significance in subnucleus interpolaris. In nucleus principalis the deprived territory was only partially activated and the degree of metabolic activation was less than in the subnuclei. In the thalamic ventrobasal complex of mice with lesions metabolic activity was unpatterned whereas two areas of metabolic activation were distinct in controls. Hence, the removal of whisker follicles in newborn mice resulted in the suppression of localized metabolic responses to whisker stimulation in the thalamus, whereas in the brainstem stimulus-related activity was prominent and the deprived territory became responsive to the stimulation of whisker follicles adjacent to the lesion. Apparently, the modification of the whisker representation at the first synapse of the pathway induces a diminution of localized responsivity in the thalamus.

Introduction

The whiskers on the snout of the mouse are topologically represented by morphological units at all synaptic relays of the ascending somatosensory pathway. Brain sections stained for the mitochondrial enzymes succinic dehydrogenase (Belford and Killackey, 1979; Durham and Woolsey, 1984) and cytochrome oxidase (Wong-Riley and Welt, 1980; Bates and Killackey, 1985) or Nissl substance (Woolsey and Van der Loos, 1970; Van der Loos, 1976; Ma and Woolsey, 1984) reveal these whisker representations in three nuclei of termination, the ventrobasal complex of the thalamus and the primary somatosensory cortex. In the last, whiskers are represented by cytoarchitectonic units in layer IV, named 'barrels' (Woolsey and Van der Loos, 1970). Barrels develop in the first postnatal week. If whisker follicles are destroyed shortly after birth, the barrels that were destined to represent these whisker follicles do not develop and neighbouring barrels enlarge into the vacant territory (Van der Loos and Woolsey, 1973). The vacant territory is filled less completely the later after birth the lesion is carried out (Jeanmonod *et al.*, 1981). In a previous deoxyglucose study we found that the vacant territory in the barrel cortex is metabolically activated by deflections of whiskers adjacent to the lesion (Melzer *et al.*, 1993). The present report provides evidence that early postnatal removal of whisker follicles altered the metabolic whisker map not only in the barrel cortex but also in thalamic and brainstem relay stations of the whisker-to-barrel pathway. Stimulus-related metabolic responses vanished in the ventrobasal complex of the thalamus. In brainstem subnuclei caudalis and interpolaris, the metabolic representations of the whiskers adjacent to the lesion enlarged into the deprived territory without an enlargement of the morphological representations. The observed alterations in the metabolic whisker map at the first synapse emphasize the important role that modifications of input at that level may play in the developmental plasticity of the whisker-to-barrel pathway.

Correspondence to: Carolyn B. Smith, as above

Received 18 September 1995, revised 26 March 1996, accepted 2 April 1996

Materials and methods

Animals

All procedures were in strict accordance with the US National Institutes of Health Guidelines for the Care and Use of Laboratory Animals and were approved by the Natonal Institute of Mental Health Animal Care and Use Committee. Male and female Swiss albino mice of International Charles Rivers origin (Harlan Sprague–Dawley, Indianapolis, IN) were used. Pregnant females were checked for offspring at noon daily. The follicles of the left whiskers C1, C2 and C3 were surgically removed from eight pups from one litter under anaesthesia by hypothermia between 5.5 and 7.0 h after the detection of the litter, i.e. on postnatal day 0. One pup from another litter underwent follicle removal 30.5 h after detection of the litter, i.e. on postnatal day 1. The hours between the detection of the newborn litter and the removal of whisker follicles were used to label the experiments. Ten unoperated mice served as controls.

Measurement of local rates of cerebral glucose utilization

Preparation of animals

The mice were allowed at least 6 weeks to mature fully. On the day prior to whisker stimulation, the mice were anaesthetized with halothane (~1.5% in 70% N_2O/30% O_2), and a femoral artery and vein were catheterized. The catheters were routed to the nape of the neck and coiled up under the skin. Pieces of Ni/Fe wire (0.2 mm in diameter and 2.5 mm long) were glued on left whiskers B1–3 and D1–3 ~5 mm above the skin, and the portion of the whiskers distal to the metal piece was trimmed off. All other whiskers were clipped close to the skin. A paper collar was placed around the animal's neck to prevent the animal from removing the metal pieces. The mice were allowed to recover for 16–24 h and provided with food and water *ad libitum*. Then they were anaesthetized with halothane (~2.0% in 70% N_2O/30% O_2) for <5 min, the catheters were exposed, and the animals were placed in a small cage inside an electromagnetic coil. Physiological variables were monitored prior to and during the measurement of local rates of cerebral glucose utilization ($lCMR_{glc}$) as described previously (Melzer *et al.*, 1993). Mice were allowed to rest for ~30 min, after which 2-deoxy-D-[1-^{14}C]glucose (DuPont-NEN, Wilmington, DE; specific activity 50–55 mCi/mmol, dose 120–150 μCi/kg) in ~40 μl heparinized saline was injected into the vein, and simultaneously a pulsing magnetic field was initiated in the coil, which deflected the six whiskers (Melzer *et al.*, 1985). The mice were stimulated for 45–50 min, during which timed 20 μl arterial blood samples were collected for determination of [^{14}C]deoxyglucose and glucose concentrations. The mice were then euthanized at a precisely recorded time, and the brains were removed and divided at the border between the inferior and superior colliculi. The rostral portion of the brain was split into the cortical hemispheres, and the tissue blocks were frozen in isopentane at –55°C. The cortical hemispheres were cut tangentially to the pia in 20 μm thick sections in a cryostat at –22°C. After the neocortex had been fully sectioned, the right hemispheres of six controls and six mice with lesions were oriented in a plane oblique from horizontal, and sections were cut through the thalamus. The sections of neocortex were used in a study of lesion-induced plasticity in the barrel cortex (Melzer *et al.*, 1993). The brainstems were cut transversely, and alternate series of sections were obtained. The sections were dried on a hotplate at 60°C, and one series was autoradiographed along with calibrated [^{14}C]methyl methacrylate standards on Kodak OMC1 X-ray film at 5°C and later stained for cytochrome oxidase activity (Wong-Riley and Welt, 1980); the other series was stained for Nissl substance.

Densitometry

Local rates of glucose utilization were measured in the areas representing whiskers A1–3, B1–3, C1–3, D1–3 and E1–3 in subnucleus caudalis and subnucleus interpolaris of the descending spinal tract of the trigeminal nerve on both sides. The measurements were carried out with the aid of a camera-based image analysis system (Imaging Research, St Catharines, Ontario, Canada). The areas were outlined on digitized images of cytochrome oxidase-stained sections on the basis of the circumferences of enzyme-rich segments. In cases in which the areas of interest could not be fully drawn on one section because of unclear segmentation, one or two adjacent sections were used to complete the outlines. This practice is acceptable because the segmentation remained sufficiently invariant along the caudorostral axis in the chosen regions of both subnuclei. The outlines were superimposed on the corresponding autoradiograms, and the concentration of ^{14}C in each delineated area was determined from the optical density in the autoradiogram and the optical density versus ^{14}C concentration curve derived from the calibrated plastic standards. Pixel-weighted averages of ^{14}C concentrations were determined from autoradiograms of eight to ten consecutive sections representing a 400 μm region along the caudorostral axis of a given subnucleus. Each region was chosen to represent the portion of the subnucleus in which the morphological representations of the whiskers were most distinct. In subnucleus caudalis this region ended 320 μm caudally from the caudal pole of subnucleus interpolaris. In subnucleus interpolaris the region began 320 μm rostral from its caudal pole. The rates of glucose utilization were calculated from the local concentrations of ^{14}C and the time courses of the arterial plasma specific activities by means of the operational equation of the deoxyglucose method (Sokoloff *et al.*, 1977). The mean of the pixel-weighted averages of each assessed area was taken to represent its local metabolic rate for that animal. Mean differences in metabolic rate between homeotopic areas ipsilateral (left side) and contralateral (right side) to both stimulation and the lesion were used as indicators of stimulus-related metabolic activation in subsequent statistical analyses.

Metabolic rates could not be measured in nucleus principalis and in the thalamic ventrobasal complex because of the small size of the representations in the former and the absence of clear segmentation in the latter. However, we were able to compare the patterns of metabolic activity in the two structures as well as in the subnuclei with the help of colour-coded, digitized images of autoradiograms produced by IMAGE (W. Rasband, NIMH, USPHS, Bethesda, MD).

Statistical analysis of metabolic rates

The mean metabolic rates of homeotopic areas on both sides of subnuclei caudalis and interpolaris were compared by means of one-tailed, paired Student's *t*-tests. One-tailed testing was justified because the barrel cortex of these animals consistently showed increases in metabolic activity contralateral to stimulation (Melzer *et al.*, 1993), which suggests that the metabolic rates in the subcortical synaptic relays should either remain unchanged or be elevated by stimulation. The left-to-right differences in local metabolic rate of mice with lesions were compared with those of unoperated controls by one-tailed Student's *t*-tests.

Areal measurement of whisker representations

In nucleus principalis of the seven mice whose whisker follicles were removed on postnatal day 0, the areas of left whisker representations B1–3 and D1–3, the deprived territory and right whisker representations B1–3, D1–3 and C1–3 were measured on transverse sections

stained for cytochrome oxidase activity. The measurements were carried out on digitized images of the sections with a camera-based image analysis system (Bioquant; R & M Biometrics Inc., Nashville, TN) fitted on a microscope (Ortholux; Leitz, Wetzlar, FRG) with a 10× objective (NPL Fluotar; Leitz). The enzyme-rich segments representing the three whisker follicles in each row were outlined as one area. The area of low enzyme activity between rows B and D ipsilateral to the lesion was outlined as the deprived territory. For each animal, between six and 19 measurements could be obtained to determine the areas' mean sizes. Side-to-side differences between homeotopic areas were analysed by means of two-tailed, paired Student's *t*-tests.

Results

In the transverse sections of subnuclei caudalis and interpolaris stained for cytochrome oxidase each whisker is represented by an enzyme-rich segment, separated from the others by a thin strip of low enzyme activity (Figs 1 and 2, left columns). The segments were frequently spliced by criss-crossing bundles of myelinated fibres. Yet the five rows representing the tall whiskers remained distinctive, and the areas of interest for the measurement of rates of glucose utilization could be identified satisfactorily. In mice with lesions, the pattern of cytochrome oxidase staining in subnuclei caudalis and interpolaris ipsilateral to the lesion was markedly different from that of the controls (Figs 1 and 2, left columns). Whereas the enzyme-rich segments representing the whiskers adjacent to the lesion did not differ remarkably from normal in shape, size and staining intensity, deprived whisker representations C1–3 stained faintly for cytochrome oxidase activity and stood out in clear contrast to the neighbouring segments. On the side contralateral to the lesion no such difference could be seen.

Subnucleus caudalis

The metabolic activity in subnucleus caudalis of mice with lesions and of controls was changed drastically by the deflection of whiskers B1–3 and D1–3. Metabolic activity was increased ipsilateral to stimulation whereas it remained low on the contralateral side (Fig. 1, right column, and Fig. 3). In both controls and mice with lesions the metabolic rates of all five assessed areas ipsilateral to stimulation were significantly higher (paired Student's *t*-test, one-tailed, $2 \times 10^{-5} < P < 0.015$) than the rates contralateral to stimulation. The mean left–right differences in metabolic rate were greatest in the appropriate representations of the stimulated whiskers, i.e. representations B1–3 and D1–3, and lowest in inappropriate whisker representations A1–3 and E1–3 (Fig. 3). In mice with lesions, the left–right difference in metabolic rate of representations C1–3, i.e. the territory deprived of sensory inputs, was ~1.5-fold greater than that of controls. This was the only area where the left–right difference in mice with lesions was significantly greater than that of controls ($P = 0.027$).

With increasing time between birth and the removal of whisker follicles the total area of metabolic activation in subnucleus caudalis seemed to become smaller and more restricted to the representations of the stimulated whisker follicles (Fig. 1).

Subnucleus interpolaris

As in subnucleus caudalis, the deflection of whiskers B1–3 and D1–3 led to a distinct increase in metabolic activity of subnucleus interpolaris ipsilateral to the stimulation (Figs 2 and 3). The stimulus produced a significant increase (paired Student's *t*-test, one-tailed) in metabolic rate of all five assessed areas on the ipsilateral side compared with that on the contralateral side in mice with lesions ($9 \times 10^{-4} \leq P \leq 0.015$) and in controls ($5 \times 10^{-5} \leq P \leq 0.049$). The greatest left–right differences in metabolic rate were found in whisker representations B1–3 and D1–3 both in controls and in mice with lesions (Fig. 3). In representations A1–3 and E1–3 the left–right differences were smallest. In mice with lesions left–right differences in metabolic activity were greater (one-tailed *t*-test) than those in controls in representations C1–3 ($P = 0.064$), D1–3 ($P = 0.071$) and E1–3 ($P = 0.084$), and smaller than those in controls in representations B1–3 ($P = 0.103$). These differences between controls and mice with lesions approached statistical significance.

Nucleus principalis

In cytochrome oxidase-stained sections the five rows of enzyme-rich segments representing the tall whiskers were well differentiated. As in the subnuclei, the segments are separated by thin bands of low enzyme activity. The enzyme activity was decreased in the territory deprived by the lesion (Fig. 4, left column) whereas it remained at normal levels in adjacent rows B and D. However, these rows appeared deformed and less parcellated in five of the seven animals which had the follicles removed on postnatal day 0. In the other mice their appearance was normal. Whisker representations B1–3 and D1–3 were on average 24 and 31%, respectively, larger than the homeotopic areas contralateral to the lesion. In contrast, the deprived territory was 52% smaller than contralateral whisker representations C1–3. These effects were significant (paired Student's *t*-test, two-tailed) in whisker representations D1–3 ($P = 0.018$) and C1–3 ($P = 0.0006$).

In mice with lesions as well as in controls the deflection of left whiskers B1–3 and D1–3 increased metabolic activity in nucleus principalis ipsilateral to stimulation (Fig. 4, right column). The areas of activation were situated laterally and ventrally in the nucleus and comprised the cytochrome oxidase-rich segments representing the deflected whiskers. In controls the greatest metabolic activation was located in segment rows B and D, with some spread into row C. In mice with lesions, stimulus-related metabolic activity seemed generally lower than in unoperated mice. Particularly, row D was less activated than row B. The deprived territory was metabolically activated, but the activation was restricted to the ventrolateral boundary of that row. Because of the small size of the whisker representations we did not attempt to quantify metabolic rates.

Ventrobasal complex

We could not distinguish barreloids in Nissl preparations from either mice with lesions or controls. In cytochrome oxidase-stained preparations the ventrobasal complex appeared as a darkly stained fractured ovoid (Fig. 5, left column). Enzyme-rich rows could be discerned only rarely (Fig. 5, CTR), and their appearance was not related to the lesion.

In five of the six controls, in which sections through the thalamus were prepared, stimulation of whiskers B1–3 and D1–3 resulted in two separate areas of increased metabolic activity (Fig. 5, right column). In the six mice with lesions, metabolic activity remained uniform throughout the nucleus. Local metabolic rates were not measured because of the lack of histological landmarks.

Discussion

The results of the present study demonstrate that a restricted irreversible lesion in the somatosensory periphery executed shortly after birth

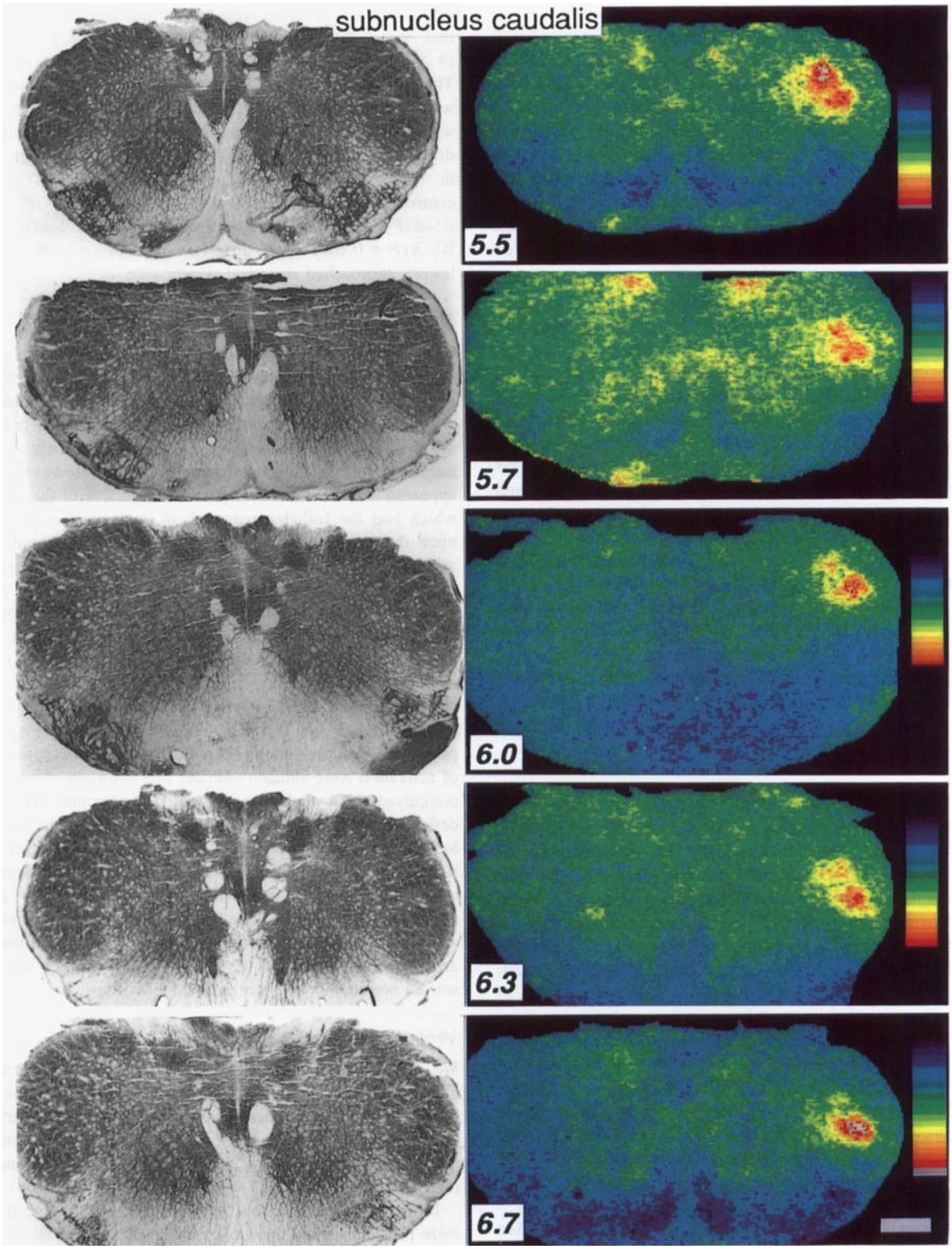

leads to the invasion of the representation of intact soma surrounding the lesion into the deprived territory already at the first synapse in the brainstem. In the thalamic ventrobasal complex, however, localized stimulus-related metabolic activity was lost. In a preceding report we had shown that the metabolic whisker map in the barrel cortex of the same mice also adapted to the loss of sensory input by invasion of the representation of the intact soma surrounding the lesion into the deprived territory (Melzer *et al.*, 1993). Similarly, infraorbital nerve transection in neonates leads to an enlargement of the representations of the soma innervated by the ophthalmic and mandibular nerves in both brainstem and cortex (Waite, 1984). This plasticity is analogous to that of the hand representation in the somatosensory cortex of

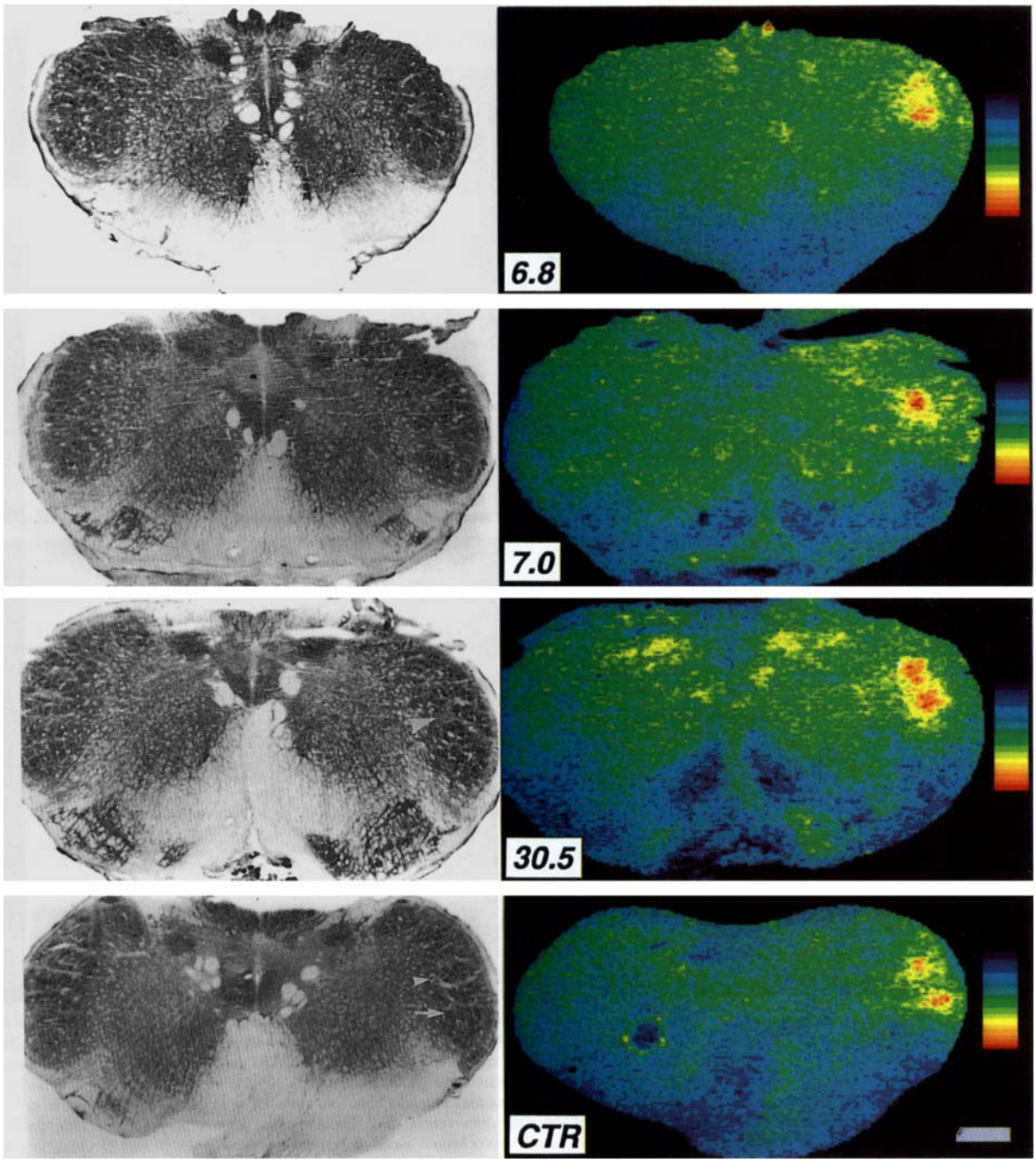

FIG. 1. Morphological whisker maps and metabolic activation patterns in subnucleus caudalis. The follicles of left whiskers C1, C2 and C3 were surgically removed shortly after birth. After the animals had reached adulthood, whiskers B1–3 and D1–3 adjacent to the lesion were deflected in a deoxyglucose study. (Left column) Transverse sections (20 μm thick) stained for cytochrome oxidase activity after autoradiography. (Right column) Colour-coded images of the autoradiograms taken from the sections. The panels are ordered by increasing time (hours) between the detection of the newborn litter and the removal of whisker follicles (shown at the lower middle of each row). CTR is an unoperated control. The whiskers are represented topologically by segments of high cytochrome oxidase activity separated by thin bands of low enzyme activity. The segments representing the five rows of tall whiskers on the snout of the mouse are prominent. Woolsey and Van der Loos (1970) designated the rows of whiskers A (dorsal) to E (ventral) and numbered each whisker beginning caudally with 1. Four single whiskers, α to γ, straddle the rows caudally. In subnucleus caudalis, row A is represented ventrally and row E dorsally. The caudal whiskers are represented medially. In CTR the arrow and arrowhead point at the segments representing whiskers B1 and D1 respectively. In mice with lesions the segments deprived by the lesion stain faintly for cytochrome oxidase activity (arrowhead in 30.5). In the images obtained with the deoxyglucose method, the metabolic activation is proportional to [^{14}C]deoxyglucose-6-phosphate accumulation, the degree of which is expressed by the colours in the bar on the right of each image (white/red is high, blue is low). Comparable colour-coding was achieved by setting the lowest optical densities in the autoradiograms to blue and the highest optical densities in the nuclei of interest to red, while keeping the number of colours equal. Excepting B1–3 of 6.7 and 7.0, the deflection of whiskers B1–3 and D1–3 increased metabolic activity to the highest degree in the appropriate representations of these whiskers, i.e. ipsilateral segments B1–3 and D1–3. Adjacent inappropriate whisker representations were activated at a lower level. Metabolic activity in segments C1–3 remained low in CTR whereas in mice with lesions this area was activated, except in 5.5, 5.7 and 30.5, less than segments B1–3 and D1–3. The total area of activation seems smaller and more restricted to the representations of the stimulated whisker follicles, when the whisker follicle had been removed late. Note that metabolic activity in subnucleus caudalis contralateral to stimulation remained low and comparably uniform (dorsal is up, the animal's right side is on the left; the scale bar in CTR represents 300 μm).

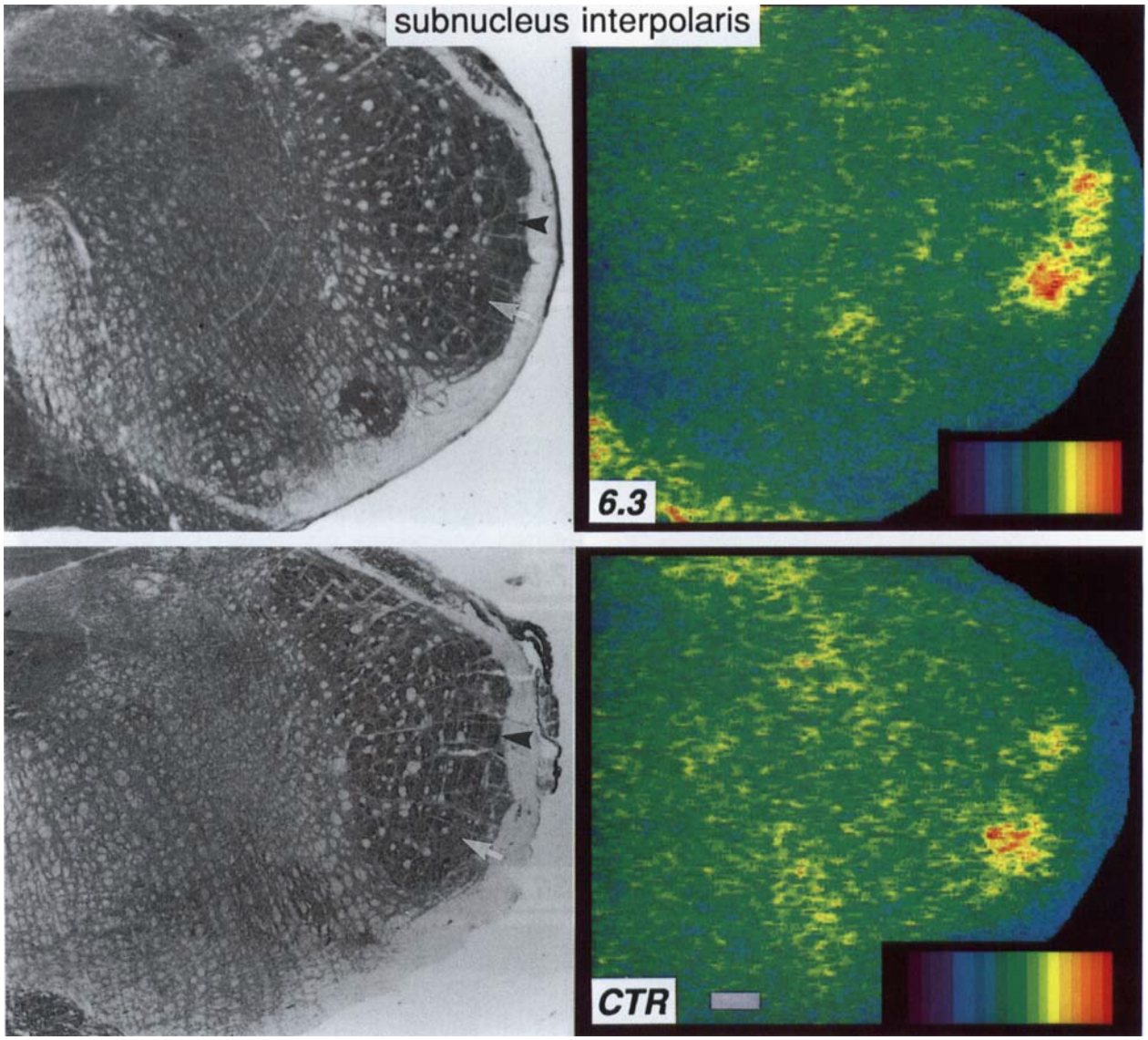

FIG. 2. Morphological whisker map and metabolic activation pattern in the left subnucleus interpolaris of the mouse, which had the follicles of left whiskers C1, C2 and C3 removed 6.3 h after the detection of its birth (6.3), and an unoperated control (CTR). Left whiskers B1–3 and D1–3 were deflected in a deoxyglucose study when the mice were 22 and 10 weeks old respectively. (Left column) Transverse sections (20 μm) stained for cytochrome oxidase activity after autoradiography. (Right column) Colour-coded images of the autoradiograms taken from the sections. In the sections stained for cytochrome oxidase activity, enzyme-rich segments represent the whiskers topologically. As in subnucleus caudalis, the five rows of segments representing the tall whiskers are distinct. However, the whisker map in subnucleus interpolaris is reversed about the dorsoventral axis. The arrow and arrowhead point at the segments representing whiskers B1 and D1 respectively. In the mouse with lesion, the area low in cytochrome oxidase activity between rows B and D comprises the deprived territory. In the colour-coded images metabolic activation is expressed by the colours in the bar on the lower right of each image (white/red is high, blue is low). The deflection of whiskers B1–3 and D1–3 increased metabolic activity in the appropriate representations of these whiskers, i.e. ipsilateral segments B1–3 and D1–3. Adjacent inappropriate whisker representations were also activated, though at lower magnitude. Metabolic activity in segments C1–3 remained low in CTR whereas in the mouse with lesion this area was activated, though less than in segments B1–3 and D1–3 (dorsal is up, medial is on the left; the scale bar in CTR represents 250 μm).

adult primates after transection of the median nerve (Merzenich *et al.*, 1983). Since in the present study the lesions were carried out before the barrels develop, but after morphological whisker representations in the brainstem form, we expected the plasticity of the metabolic whisker map to be greater in the barrel cortex than in the brainstem. In contrast, our findings suggest that the plasticity of whisker representation is an equally powerful feature of the first synapse of the pathway.

Methodological considerations

For the purpose of quantification, the spatial resolution of the autoradiographic [^{14}C]deoxyglucose method was determined to be ~200 μm (Smith, 1983). Resolution is limited primarily by the diffusion of [^{14}C]deoxyglucose-6-phosphate that occurs when tissue sections are thaw-mounted. In the present study we have attempted to resolve quantitatively in subnuclei caudalis and interpolaris the metabolic activity of adjacent whisker representations that

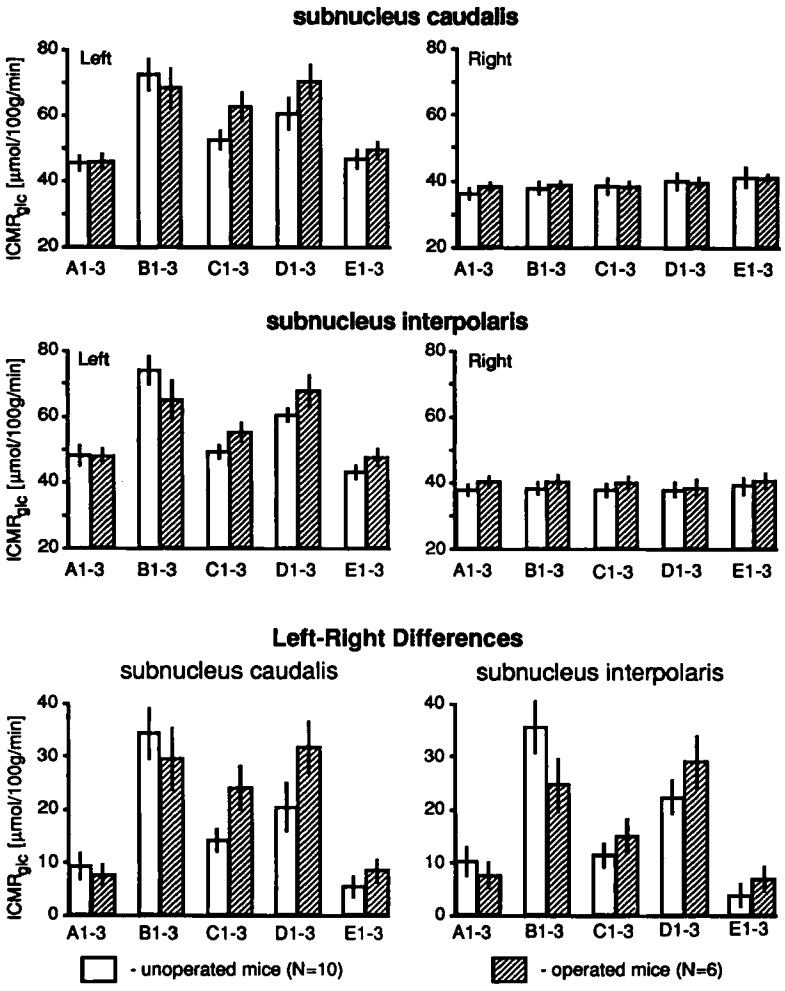

FIG. 3. Local cerebral metabolic rates of glucose utilization ($lCMR_{glc}$) in subnuclei caudalis and interpolaris. The bar graphs represent the mean metabolic rates from six mice, in which the follicles of left whiskers C1, C2 and C3 had been removed shortly after birth (6.0 was excluded because the metabolic rates were two standard deviations below the respective group means, and 30.5 was excluded to narrow the range of times of lesion), and ten unoperated controls. When the mice reached adulthood they were subjected to the deoxyglucose study in which left whiskers B1–3 and D1–3 were deflected. Group means (bars) and standard errors of the mean are shown for subnucleus caudalis (top) and subnucleus interpolaris (centre) as well as the mean left–right differences in metabolic rate between homeotopic areas (bottom). In operated as well as in unoperated mice, mean $lCMR_{glc}$ values in both subnuclei were highest in the areas representing deflected whiskers B1–3 and D1–3. In mice with lesions, deprived whisker representations C1–3 had greater side-to-side differences in metabolic rate than the homeotopic representations in controls. The increase reached significance in subnucleus caudalis (one-tailed Student's t-test, $P \leq 0.05$). In addition, the increase in metabolic activation of representations D1–3 as well as the changes in activation of representations B1–3, C1–3 and D1–3 in subnucleus interpolaris approached statistical significance (one-tailed Student's t-test, $0.05 \leq P \leq 0.10$).

are 70–150 µm across. The increases in $lCMR_{glc}$ of representations C1–3 in the two subnuclei and, to a lesser degree, of representations A1–3 and E1–3 may be attributed to a spill-over of [^{14}C]deoxyglucose-6-phosphate from the metabolically activated whisker representations B1–3 and D1–3. However, the stimulus-related increase in $lCMR_{glc}$ of representations C1–3 in mice with lesions was greater than in unoperated controls whereas the increases in the other two areas remained similar to the increases in the unoperated controls. This difference provides strong evidence that the neonatal removal of whisker follicles C1–3 indeed resulted in a novel responsivity of the deprived whisker representations to the stimulation of whiskers neighbouring the lesion.

Brainstem nuclei

The pattern of cytochrome oxidase-rich segments we observed in the nuclei of termination of unoperated mice on both sides and on the side contralateral to the lesion of mice with lesions is in good agreement with the patterns of succinic dehydrogenase-rich segments described by others (Belford and Killackey, 1979; Woolsey and Durham, 1984). The segments have been shown to match the clustered terminal fields of primary afferents in normal rats (Bates and Killackey, 1985; Chiaia *et al.*, 1992; Renehan *et al.*, 1994). The location of the areas of increased rates of glucose utilization within the nuclei confirms the observation that the caudal whiskers are represented at the medial boundary of subnucleus caudalis (Arvidsson, 1982; Jacquin *et al.*, 1986a) and at the lateral boundaries of subnucleus interpolaris (Arvidsson, 1982; Jacquin *et al.*, 1986b) and nucleus principalis (Bates *et al.*, 1982). In the three nuclei, row A is represented ventrally and row E dorsally. Our observations are in harmony with those of others who found that after the cauterization of a row of whisker follicles at birth the activities of mitochondrial enzymes diminish in the appropriate representations and their areas decrease in the three

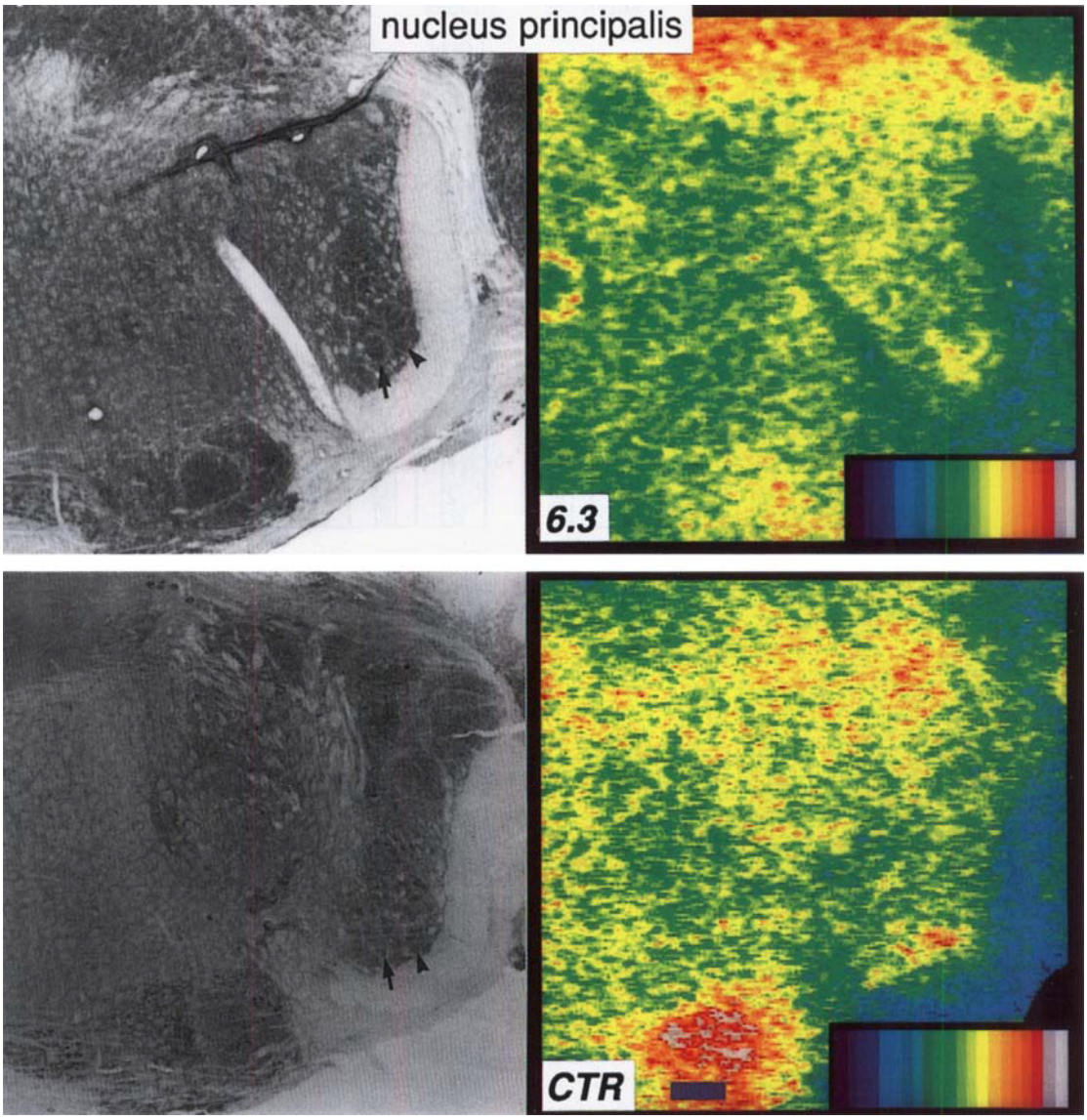

FIG. 4. Morphological whisker map and metabolic activation pattern in the left nucleus principalis of the mouse which had the follicles of left whiskers C1, C2 and C3 removed 6.3 h after the detection of its birth (6.3), and an unoperated control (CTR). Left whiskers B1–3 and D1–3 were deflected in a deoxyglucose study carried out when the mice were 22 and 10 weeks old, respectively. (Left column) Transverse sections (20 μm) stained for cytochrome oxidase activity after autoradiography. (Right column) Colour-coded images of the autoradiograms taken from the sections. Like subnuclei caudalis and interpolaris, nucleus principalis contains a topological whisker map. In the sections stained for cytochrome oxidase activity, the representations of the five rows of tall whiskers are clearly distinguishable as rows of enzyme-rich segments. As in subnucleus interpolaris, caudal whiskers are represented laterally. The arrow and arrowhead point at the segments representing whiskers B1 and D1 respectively. In the mouse with lesion, the band low in cytochrome oxidase activity between rows B and D comprises the territory deprived by the lesion. This band is narrower in width than the corresponding area in CTR, and the adjacent segments in row B and D seem abnormal in shape and less separated. In the colour-coded images metabolic activation is expressed by the colours in the bar on the lower right of each image (white/red is high, blue is low). The deflection of whiskers B1–3 and D1–3 increased metabolic activity roughly in the appropriate loci, i.e. lateral rows B and D ipsilateral to stimulation. In CTR metabolic activation spread slightly from these rows into the adjacent rows. In the mouse with lesion, deprived C1–3 seemed partially activated, while metabolic activity in row D was distinctly less than in row B (dorsal is up, medial is on the left; the scale bar in CTR represents 250 μm).

brainstem structures ipsilateral to the lesion (Belford and Killackey, 1980; Woolsey and Durham, 1984; Bates and Killackey, 1985; Rhoades *et al.*, 1989; Renehan *et al.*, 1989; Chiaia *et al.*, 1992b).

Subnuclei caudalis and interpolaris

We did not find regenerated myelinated nerve fibres at the site of the lesion, nor could we detect any increase in the number of nerve fibres innervating whisker follicles neighbouring the lesion (Melzer *et al.*, 1993). In fact, we found several follicles with diminished innervation. Similarly, after transection of the infraorbital branch of the trigeminal nerve in newborn rats, the number of nerve fibres in the infraorbital nerve drastically decreases (Waite, 1984; Klein *et al.*, 1988). Moreover, neuronal death increases in the Gasserian ganglion (Klein *et al.*, 1988) and in the nuclei of termination (Waite, 1984; Ashwell and Waite, 1991). Therefore, in the present study ganglion cells, which were axotomized by the follicle removal, may have died in such great

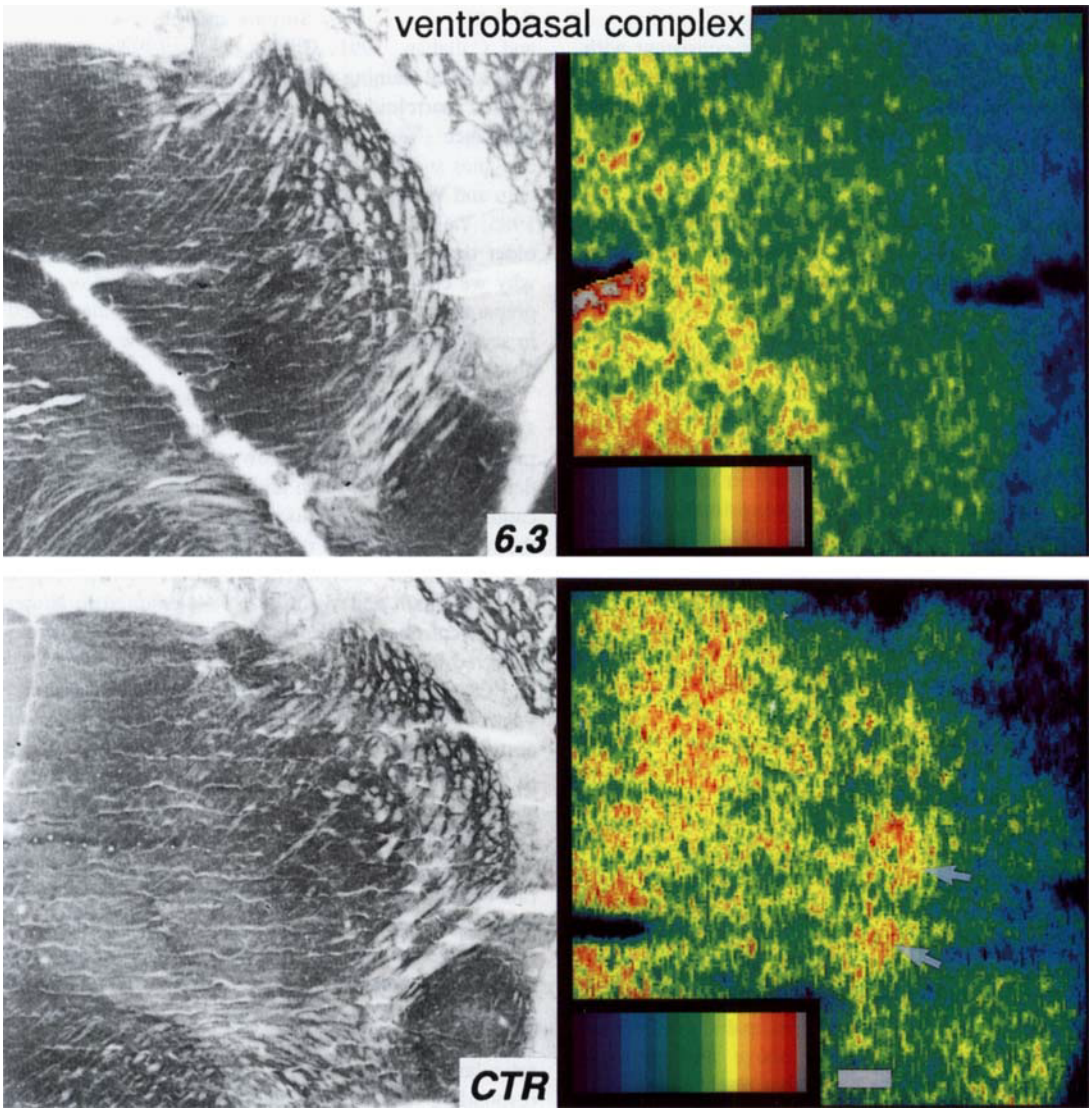

FIG. 5. Morphology and metabolic activation pattern in the ventrobasal complex of the right thalamus of the mouse, which had the follicles of left whiskers C1, C2 and C3 removed 6.3 h after detection of its birth (6.3) and an unoperated control (CTR). Left whiskers B1–3 and D1–3 were deflected in a deoxyglucose study carried out when the mice were 22 and 10 weeks old, respectively. (Left column) Sections (20 μm) cut obliquely to the horizontal plane and stained for cytochrome oxidase activity after autoradiography. (Right column) Colour-coded images of the autoradiograms taken from the sections. In the sections stained for cytochrome oxidase activity, no morphological whisker map could be discerned. The nucleus appears as darkly stained patches forming an ovoid near the centre of the micrographs. In the colour-coded images metabolic activation is expressed by the colours in the bar on the lower left of each image (white/red is high, blue is low). In CTR, two separate areas of metabolic activity can be distinguished (arrows). In the mouse with the lesion, metabolic activity was uniform (rostral is up, lateral is on the right; the scale bar in CTR represents 250 μm).

number that the corresponding sites of termination in the brainstem were depleted of the original afferents, and the postsynaptic elements decreased in cytochrome oxidase activity (Wong-Riley, 1989).

However, the metabolic responsivity to the stimulation of whisker follicles adjacent to the lesion increased in the deprived territory of the two subnuclei, which points to a mechanism to compensate for the loss of input at the first synapse of the pathway. An explanation may be provided by the finding that primary afferents in subnucleus interpolaris extend arbors beyond the appropriate areas of termination into the territory deprived by neonatal cauterization of rows of whisker follicles (Renehan *et al.*, 1994). Interestingly, this expansion occurs at a time past embryonic day 18 on which the period of plasticity for the enlargement of mitochondrial enzyme-rich segments ends (Chiaia *et al.*, 1992a). An expansion of the endings of primary afferents from the whisker follicles adjacent to the lesion without an enlargement of cytochrome oxidase-rich segments may, therefore, underlie the increase in metabolic responsivity in the deprived territory we observed.

This increase in metabolic responsivity was greater in subnucleus caudalis than in subnucleus interpolaris. Similarly, the terminal fields of primary afferents enlarge more in subnucleus caudalis (Jacquin *et al.*, 1986a) than in subnucleus interpolaris (Renehan *et al.*, 1989) after transection of the infraorbital nerve in neonatal rats. The difference in metabolic responsivity to stimulation in the deprived territory between the two subnuclei may reflect a difference in the capacity of primary afferents to elongate into that territory during postnatal development. The trend we observed in subnucleus caudalis for the total area of metabolic activation to be larger the earlier the

lesion had been carried out may indicate that there is a limited period for plasticity of functional maps. This conclusion is consistent with the notion of critical periods of plasticity of morphological maps in the whisker-to-barrel pathway (Belford and Killackey, 1980; Jeanmonod *et al.*, 1981; Durham and Woolsey, 1984).

Nucleus principalis

The change in area, shape and segmentation of the mitochondrial enzyme-rich rows adjacent to the deprived territory we observed in nucleus principalis was not noted in studies in which whisker follicles were cauterized (Belford and Killackey, 1980; Durham and Woolsey, 1984; Bates and Killackey, 1985; Chiaia *et al.*, 1991). Cytochrome oxidase-rich segments in nucleus principalis only enlarged when whisker follicles were cauterized in more than one row and before embryonic day 18 (Chiaia *et al.*, 1992a). With cautery, the destruction of the follicles often remains incomplete and the surviving follicles may be innervated (Jeanmonod *et al.*, 1981; Durham and Woolsey, 1984). Moreover, the deprived territory still receives primary afferents connected to damaged follicles (Renehan *et al.*, 1994). In contrast, in the present study the follicles were surgically removed. Some mice had follicular remnants at the site of the lesion, but when the lesion was carried out on postnatal day 0 the remnants did not receive deep innervation (Melzer *et al.*, 1993). Only the complete deprivation of the peripheral innervation may, therefore, lead to changes in size and segmentation.

Cytochrome oxidase-rich segments in nucleus principalis may be more plastic than those in the subnuclei. In the rat, subnucleus interpolaris segmentation develops between embryonic days 19 and 20 (Chiaia *et al.*, 1992a) whereas in nucleus principalis clear segmentation is gained only at birth, i.e. embryonic day 21 (Bates *et al.*, 1982; Chiaia *et al.*, 1992a). Following the transection of the infraorbital nerve at birth, segmentation shows earlier signs of disintegration (Chiaia *et al.*, 1992b), and neuronal death is greater in nucleus principalis than in the subnuclei (Waite, 1984; Chiaia *et al.*, 1992b). In addition, naturally occurring neuronal death during postnatal development is slightly greater in nucleus principalis than in the subnuclei (Ashwell and Waite, 1991). The above findings may advocate a higher degree of immaturity in this nucleus at birth. Consistent with a caudorostral sequence of maturation, the onset of stimulus-related metabolic activation in nucleus principalis lags behind that in the two subnuclei (Melzer *et al.*, 1994). Because of the late maturation the critical period of plasticity may end later in nucleus principalis.

In unoperated controls, metabolic activation in rows B and D was less restricted to the appropriate enzyme-rich segments than in the two subnuclei, though the two areas of activation remained distinctly separated. In contrast, metabolic activation stretched across the deprived territory in mice with lesions. Indeed, in rats with neonatal follicle cautery primary afferents from intact whisker follicles adjacent to the lesion were observed to extend into inappropriate locations (Renehan *et al.*, 1994). However, the metabolic enzyme-rich segments did not enlarge. It remains puzzling that we found greater plasticity in segmentation in nucleus principalis than in the subnuclei while the changes in the metabolic whisker map seemed smaller. Perhaps the elongation of primary afferents in response to a lesion in the sensory periphery is a mechanism available only after the critical period for segmentation has ceased. Because the gestational period of mice is up to 2 days shorter than that of rats, this may not have been the case at the time of the lesion in the present study.

Ventrobasal complex

The ventrobasal complex of the thalamus contains a somatotopic map demonstrable with single- and multi-unit recordings (Waite, 1973; Rhoades *et al.*, 1987; Simons and Carvell, 1988; Armstrong-James and Callahan, 1991; Chiaia *et al.*, 1992b; Lee *et al.*, 1994) and histological staining methods. Morphological whisker representations, termed barreloids, can be distinguished with staining for Nissl substance (Van der Loos, 1976) as well as for the mitochondrial enzymes succinic dehydrogenase (Belford and Killackey, 1979; Durham and Woolsey, 1984) and cytochrome oxidase (Land and Simons, 1985; Yamakado, 1985). However, barreloids disintegrate in animals older than 2 weeks (Ivy and Killackey, 1982), which may explain why we could not discern any in either Nissl or cytochrome oxidase preparations. We could, however, localize the nucleus satisfactorily in sections stained for cytochrome oxidase activity, though we could not determine its precise boundaries.

Metabolic mapping of the ventrobasal complex showed two distinct areas of metabolic activity in unoperated controls. Their orientation matched with that of the rows of barreloids shown by others (Van der Loos, 1976; Durham and Woolsey, 1984; Yamakado, 1985). The caudal area is roughly located where whisker row B is represented; the rostral area where row D is represented. Early cauterization of a row of whisker follicles in rats (Belford and Killackey, 1980) and mice (Durham and Woolsey, 1984) resulted in altered segmentation in the ventrobasal complex and a decrease in enzyme activity in the deprived territory. In the present study deflections of whiskers B1–3 and D1–3 did not result in distinct loci of metabolic activity in the ventrobasal complex of mice with lesions. In contrast, the barrel cortex of these animals showed circumscribed, distinctive increases in metabolic activity in the areas representing the deflected whiskers as well as in the territory deprived by the lesion (Melzer *et al.*, 1993). Jacquin (1989) reported that the somatotopic organization of thalamic projection neurons in the brainstem had greatly deteriorated in adult rats with neonatal infraorbital nerve transection, and it may well have been perturbed in the present study. A decrease in somatotopic specificity could result in a greater divergence of corticofugal projections to the thalamus from the barrel cortex (Hoogland *et al.*, 1988; Chmielowska *et al.*, 1989) and a less specific inhibitory input from the reticular nucleus (DeBiasi *et al.*, 1988). Excitotoxic lesion of the reticular nucleus in the rat enlarged the receptive fields of neurons responding to whisker deflections in the ventrobasal complex by an average of 3.2-fold (Lee *et al.*, 1994), and a less effective input from reticular nucleus may have caused the uniform metabolic activity we observed in mice with lesions.

Outlook

The removal of three whisker follicles in newborn mice resulted in the enlargement of the metabolic representations of the whiskers adjacent to the lesion into the deprived territory in the nuclei of termination of the primary afferents. We attributed the newly acquired responsivity to the expansion of the primary afferents from intact whisker follicles into the deprived territory. This important hypothesis must be tested in future studies, particularly because changes in the action of local interneurons, projection neurons and corticofugal connections may also contribute to the plasticity of metabolic whisker maps.

Surprisingly, differentiable metabolic responses vanished in the thalamic ventrobasal complex of mice with lesions. Since we showed earlier that the metabolic whisker map in the barrel cortex was very prominent and changed in a manner similar to those in the brainstem (Melzer *et al.*, 1993), the ventrobasal complex must have conveyed the instructions for change from the nuclei of termination to the barrel cortex. A possible explanation is that a strong inhibitory mechanism could have been imposed on the metabolic activation pattern in the ventrobasal complex to suppress the manifestation of

locally differentiable effects of the lesion, as found in the synaptic relays lower and higher in the pathway, and this hypothesis merits further study.

Acknowledgements

P. M. was supported by a Fogarty Fellowship. We are indebted to T. P. Dang, Y. Sun and K. Schmidt for their help in critical phases of the experiments, A. Tannenbaum, J. Jehle, V. TenEyck and E. Lewis for technical assistance, and J. D. Brown for photography. We are indebted to Prof. H. Van der Loos, Institute of Anatomy, University of Lausanne, Switzerland, for providing the stimulator, to Prof. K. G. Götz, Max-Planck-Institut für biologische Kybernetik, Tübingen, Germany, for providing the wire used for the deflection of the whiskers, and to Prof. J. A. McKanna, Vanderbilt University, Nashville, TN, for the use of Bioquant. We thank L. Sokoloff for many helpful comments and his unrelenting support.

Abbreviations

$lCMR_{glc}$ local rate of cerebral glucose utilization

References

Armstrong-James, M. and Callahan, C. A. (1991) Thalamo-cortical processing of vibrissal information in the rat: II. Spatiotemporal convergence in the thalamic ventroposterior medial nucleus (VPm) and its relevance to generation of receptive fields of S1 cortical 'barrel' neurons. *J. Comp. Neurol.*, **303**, 211–224.

Arvidsson, J. (1982) Somatotopic organization of vibrissae afferents in the trigeminal sensory nuclei of the rat studied by transganglionic transport of HRP. *J. Comp. Neurol.*, **211**, 84–92.

Ashwell, K. W. S. and Waite, P. M. E. (1991) Cell death in the developing trigeminal nuclear complex of the rat. *Dev. Brain Res.*, **63**, 291–295.

Bates, C. A. and Killackey, H. P. (1985) The organization of the neonatal rat's brainstem trigeminal complex and its role in the formation of central trigeminal patterns. *J. Comp. Neurol.*, **240**, 265–287.

Bates, C. A., Erzurumlu, R. S. and Killackey, H. P. (1982) Central correlates of peripheral pattern alterations in the trigeminal system of the rat. III. Neurons of the principal sensory nucleus. *Brain Res.*, **281**, 108–113.

Belford, G. R. and Killackey, H. P. (1979) The development of vibrissae representation in subcortical trigeminal centers of the neonatal rat. *J. Comp. Neurol.*, **188**, 63–74.

Belford, G. R. and Killackey, H. P. (1980) The sensitive period in the development of the trigeminal system of the neonatal rat. *J. Comp. Neurol.*, **193**, 335–350.

Chiaia, N. L., Rhoades, R. W., Bennett-Clarke, C. A., Fish, S. E. and Killackey, H. P. (1991) Thalamic processing of vibrissal information in the rat: II. Morphological and functional properties of medial ventral posterior nucleus and posterior nucleus neurons. *J. Comp. Neurol.*, **314**, 217–236.

Chiaia, N. L., Bennett-Clarke, C. A., Eck, M., White, F. A., Crissman, R. S. and Rhoades, R. W. (1992a) Evidence for prenatal competition among the central arbors of trigeminal primary afferent neurons. *J. Neurosci.*, **12**, 62–76.

Chiaia, N. L., Bennett-Clarke, C. A. and Rhoades, R. W. (1992b) Differential effects of peripheral damage upon vibrissa-related patterns in trigeminal nucleus principalis and subnuclei interpolaris and caudalis. *Neuroscience*, **49**, 141–156.

Chmielowska, J., Carvell, G. E. and Simons, D. J. (1989) Spatial organization of thalamocortical and corticothalamic projection systems in the rat SmI barrel cortex. *J. Comp. Neurol.*, **285**, 325–338.

DeBiasi, S., Frassoni, C. and Spreafico, R. (1988) The intrinsic organization of the ventroposterolateral nucleus and related reticular thalamic nucleus of the rat: a double-labeling ultrastructural investigation with γ-aminobutyric acid immunogold staining and lectin-conjugated horseradish peroxidase. *Somatosens. Res.*, **5**, 187–203.

Durham, D. and Woolsey, T. A. (1984) Effects of neonatal whisker lesions on mouse central trigeminal pathway. *J. Comp. Neurol.*, **223**, 424–447.

Hoogland, P. V., Welker, E. and Van der Loos, H. (1988) Organization of the projections from barrel cortex to thalamus in mice studied with *Phaseolus vulgaris*-leucoagglutinin and HRP. *Exp. Brain Res.*, **68**, 73–87.

Ivy, G. O. and Killackey, H. P. (1982) Ephemeral cellular segmentation in the thalamus of the neonatal rat. *Dev. Brain Res.*, **2**, 1–17.

Jacquin, M. F. (1989) Structure–function relationships in rat brainstem subnucleus interpolaris. V. Functional consequences of neonatal infraorbital nerve section. *J. Comp. Neurol.*, **282**, 63–79.

Jacquin, M. F., Renehan, W. E., Mooney, R. D. and Rhoades, R. W. (1986a) Structure–function relationships in rat medullary and cervical dorsal horns. I. Trigeminal primary afferents. *J. Neurophysiol.*, **55**, 1153–1186.

Jacquin, M. F., Woerner, D., Szczepanik, A. M., Riecker, V., Mooney, R. D. and Rhoades, R. W. (1986b) Structure–function relationships in rat brainstem subnucleus interpolaris. I. Vibrissa primary afferents. *J. Comp. Neurol.*, **243**, 266–279.

Jacquin, M. F., Wiegand, M. R. and Renehan, W. E. (1990) Structure–function relationships in rat brainstem subnucleus interpolaris. VIII. Cortical inputs. *J. Neurophysiol.*, **64**, 3–27.

Jeanmonod, D., Rice, F. L. and Van der Loos, H. (1981) Mouse somatosensory cortex: alterations in the barrelfield following receptor injury at different early postnatal ages. *Neuroscience*, **6**, 1503–1535.

Klein, B. G., Renehan, W. E., Jacquin, M. F. and Rhoades, R. W. (1988) Anatomical consequences of neonatal infraorbital nerve transection upon the trigeminal ganglion and vibrissa follicle nerves in the adult rat. *J. Comp. Neurol.*, **268**, 469–488.

Land, P. W. and Simons, D. J. (1985) Metabolic and structural correlates of the vibrissae representation in the thalamus of the adult rat. *Neurosci. Lett.*, **60**, 319–324.

Lee, S. M., Friedberg, M. H. and Ebner, F. F. (1994) The role of GABA-mediated inhibition in the rat ventral posterior medial thalamus. I. Assessment of receptive field changes following thalamic reticular nucleus lesions. *J. Neurophysiol.*, **71**, 1702–1715.

Ma, P. and Woolsey, T. A. (1984) Cytoarchitectonic correlates of the vibrissae in the medullary trigeminal complex of the mouse. *Brain Res.*, **306**, 374–379.

Melzer, P., Van der Loos, H., Dörfl, J., Welker, E., Robert, P., Emery, D. and Berrini, J.-C. (1985) A magnetic device to stimulate selected whiskers of freely moving or restrained small rodents: its application in a deoxyglucose study. *Brain Res.*, **348**, 229–240.

Melzer, P., Crane, A. M. and Smith, C. B. (1993) Mouse barrel cortex functionally compensates for deprivation produced by neonatal lesion of whisker follicles. *Eur. J. Neurosci.*, **5**, 1638–1652.

Melzer, P., Welker, E., Dörfl, J. and Van der Loos, H. (1994) Maturation of neuronal metabolic responses to vibrissa stimulation in the developing whisker-to-barrel pathway of the mouse. *Dev. Brain Res.*, **77**, 227–250.

Merzenich, M. M., Kaas, J. H., Wall, J., Sur, M. and Felleman, D. (1983) Topographic reorganization of somatosensory cortical areas 3b and 1 in adult monkeys following restricted deafferentation. *Neuroscience*, **8**, 33–55.

Renehan, W. E., Rhoades, R. W. and Jacquin, M. F. (1989) Structure–function relationships in rat brainstem subnucleus interpolaris: VII. Primary afferent central terminal arbors in adults subjected to infraorbital nerve section at birth. *J. Comp. Neurol.*, **289**, 493–508.

Renehan, W. E., Crissman, R. S. and Jacquin, M. F. (1994) Primary afferent plasticity following partial denervation of the trigeminal brainstem nuclear complex in the postnatal rat. *J. Neurosci.*, **14**, 721–739.

Rhoades, R. W., Belford, G. R. and Jacquin, M. F. (1987) Receptive-field properties of rat ventral posterior medial neurons before and after selective kainic acid lesions of the trigeminal brain stem complex. *J. Neurophysiol.*, **57**, 1577–1600.

Rhoades, R. W., Chiaia, N. L., Macdonald, G. J. and Jacquin, M. F. (1989) Effects of fetal infraorbital nerve transection upon trigeminal primary afferent projections in the rat. *J. Comp. Neurol.*, **287**, 82–97.

Simons, D. J. and Carvell, G. E. (1988) Thalamocortical response in the rat vibrissa/barrel system. *J. Neurophysiol.*, **61**, 311–330.

Smith, C. B. (1983) Localization of activity-associated changes in metabolism of the central nervous system with the deoxyglucose method: prospects for cellular resolution. In Barker, J. L. and McKelvy, J. F. (eds), *Current Methods in Cellular Neurobiology. Vol. I: Anatomical Techniques.* J. Wiley & Sons, New York, pp. 268–317.

Sokoloff, L., Reivich, M., Kennedy, C., Des Rosier, D. H., Patlak, C. S., Pettigrew, K. D., Sakurada, O. and Shinohara, M. (1977) The [^{14}C]deoxyglucose method for the measurement of local cerebral glucose utilization: theory, procedure and normal values in the conscious and anesthetized albino rat. *J. Neurochem.*, **28**, 897–916.

Van der Loos, H. (1976) Barreloids in mouse somatosensory thalamus. *Neurosci. Lett.*, **2**, 1–6.

Van der Loos, H. and Woolsey, T. A. (1973) Somatosensory cortex: structural alterations following early injury to sense organs. *Science*, **179**, 395–397.

Waite, P. M. E. (1973) The responses of cells in the rat thalamus to mechanical movements of whiskers. *J. Physiol. (Lond.)*, **228**, 541–561.

Waite, P. M. E. (1984) Rearrangement of neuronal responses in the trigeminal system of the rat following peripheral nerve section. *J. Physiol. (Lond.)*, **352**, 425–445.

Wong-Riley, M. T. T. (1989) Cytochrome oxidase: an endogenous metabolic marker for neuronal activity. *Trends Neurosci.*, **12**, 94–101.

Wong-Riley, M. T. T. and Welt, C. (1980) Histochemical changes in cytochrome oxidase activity of cortical barrels after vibrissal removal in neonatal and adult mice. *Proc. Natl Acad. Sci. USA*, **77**, 2333–2337.

Woolsey, T. A. and Van der Loos, H. (1970) The structural organization of layer IV in the somatosensory region (SMI) of mouse cerebral cortex. The description of a cortical field composed of discrete cytoarchitectonic units. *Brain Res.*, **17**, 205–242.

Yamakado, M. (1985) Postnatal development of barreloid neuropils in the ventrobasal complex of mouse thalamus: a histochemical study for cytochrome oxidase. *Brain Nerve*, **37**, 497–506.